Low-Magnitude Mechanical Loading Becomes Osteogenic When Rest Is Inserted Between Each Load Cycle

SUNDAR SRINIVASAN[1], **DAVID A. WEIMER**[2], **STEVEN C. AGANS**[1], **STEVEN D. BAIN**[3], and **TED S. GROSS**[1]

1 *Orthopedic Science Laboratories, Department of Orthopedics and Sports Medicine, University of Washington, Seattle, Washington, USA.*

2 *Department of Orthopedics, University of Cincinnati, Cincinnati, Ohio, USA.*

3 *SkeleTech, Inc., Bothell, Washington, USA.*

Abstract

Strategies to counteract bone loss with exercise have had fairly limited success, particularly those regimens subjecting the skeleton to mild activity such as walking. In contrast, here we show that it is possible to induce substantial bone formation with low-magnitude loading. In two distinct in vivo models of bone adaptation, we found that insertion of a 10-s rest interval between each load cycle transformed a locomotion-like loading regime that minimally influenced osteoblast activity into a potent anabolic stimulus. In the avian ulna model, the minimal mean (+SE) periosteal labeled surface (Ps.LS) observed in the intact contralateral bones ($1.6 \pm 1.5\%$) was doubled after 3 consecutive days of low-magnitude loading ($3.8 \pm 1.5\%$; $p = 0.03$). However, modifying the regimen by inserting 10 s of rest between each load cycle significantly enhanced the periosteal response ($21.9 + 4.5\%$; $p = 0.03$). In the murine tibia model, 5 consecutive days of 100 low-magnitude loading cycles did not significantly alter mean periosteal bone formation rate (BFR) compared with contralateral bones ($0.011 \pm 0.005\ \mu m^3/\mu m^2$ per day vs. $0.021 \pm 0.013\ \mu m^3/\mu m^2$ per day). In contrast, separating each of 10 of the same loading cycles with 10 s of rest significantly elevated periosteal BFR ($0.167 \pm 0.049\ \mu m^3/\mu m^2$ per day; $p = 0.01$). Endocortical bone formation parameters were not altered by any loading regimen in either model. We conclude that 10 s of rest between each load cycle of a low-magnitude loading protocol greatly enhances the osteogenic potential of the regimen.

Keywords

mechanotransduction; exercise; osteoblast; bone mass; osteogenic

INTRODUCTION

Dɪᴍɪɴɪsʜᴇᴅ ʙᴏɴᴇ mass in the elderly arises because of degradation of the normal balance between bone resorption and bone formation observed in the young adult.(1,2) Current treatment strategies have focused on inhibiting bone resorption and are highly successful, particularly in blocking elevated resorption associated with menopause.(3) However, options for elevating bone formation as a means of enhancing bone mass are extremely limited.(4,5) Given our rapidly aging population, the current inability to augment safely and effectively bone mass consigns millions to a fate of elevated fracture risk for a substantial portion their lives.(6)

Mechanical loading of bone has substantial potential to induce bone formation.(7,8) However, application of exercise regimens in humans as a means of augmenting bone mass has met with mixed results.(9) The elderly, in particular, are unable to comply consistently with the high-impact strenuous loading events typically associated with even minimal bone accretion.(10) Unfortunately, lower-magnitude exercise strategies are extremely limited in their ability to enhance bone mass.(11)

A growing body of experimental data support the hypothesis that fluid flow near osteocytes underlies mechanotransduction within bone. Osteocytes reside within lacunae and canaliculi inside the mineralized matrix.(12–14) Mechanical loading greatly accentuates fluid flow and diffusion within bone(15,16) and osteocytes are highly responsive to fluid flow.(17,18) Additionally, bone formation induced by mechanical loading is spatially associated with locations of large strain gradients, which, in turn, stimulate fluid flow.(19,20) However, given the spatial dimensions of the osteocyte's lacunae and its cellular glycocalix coating, flow of fluid past the cell body and cell processes is likely to be highly viscous.(21–23) This physical consideration suggests that if bone is loaded repetitively (i.e., at typical stride frequencies of 1 Hz and higher), sufficient time may not exist for osteocyte level fluid flow to recover from inertial damping effects between each load cycle.(24) Fluid flow and thus osteocyte stimulation, therefore, potentially are much reduced after the first few cycles of repetitive loading. If so, it is likely that inserting a "sufficient" time period between each loading cycle would heighten fluid flow near osteocytes by facilitating recovery from inertial damping effects.

Therefore, we hypothesized that inserting a nonloaded rest pause between each loading cycle would increase the osteogenic potential of a low-magnitude locomotion-like mechanical loading regimen. We examined our hypothesis using both the avian ulna model and a recently developed noninvasive murine tibia model of bone adaptation. Specifically, we contrasted the ability of low-magnitude loading regimens with and without a 10-s rest interval inserted between each load cycle to induce osteoblastic activation and/or bone formation.

MATERIALS AND METHODS

Avian ulna model

In this study, eight middle-aged male turkeys (2 years old) underwent the functionally isolated avian ulna procedure.(25) The left ulna of each turkey was isolated from functional loading by parallel metaphyseal osteotomies performed on both ends of the bone. Transcutaneous Steinmann pins were passed through stainless steel caps placed over the exposed diaphyseal bone ends to enable external loading via a pneumatic actuator. After surgery, the turkeys were assigned randomly to one of two groups (standard regime or rest-inserted regime). Both groups underwent 1-week protocols. Beginning on day 3 postoperatively, the ulna was loaded externally in bending, with a strain distribution similar to that induced during moderate wing flap. For the standard regime ($n = 4$), the left ulna was loaded for 100 cycles with a 1-Hz sawtooth waveform on days 3, 4, and 5. Animals undergoing the rest-inserted regime ($n = 4$) underwent an identical waveform (same magnitude and loading rate), except that a 10-s unloaded rest pause was inserted between each of the 100 loading cycles (Fig. 1). Mineralization of osteoid associated with bone apposition at the ulnar middiaphysis was detected via administration of calcein (3 mg/kg intravenously [iv]) on day 6.

After death, 200-μm-thick sections were removed from the middiaphysis of both the experimental and the intact contralateral ulnas. The sections were hand ground to 80 μm, blinded, and imaged (100×) using a spot digital camera mounted on a Nikon diaphot epifluorescence microscope. Using mean end loading conditions established via two separate strain-gauged calibration bones,(26) beam theory was applied to the middiaphysis cross-

section geometry of each intact contralateral bone to quantify peak middiaphyseal strains induced in both experimental groups. Custom written software (PV-Wave; VNI, Inc., Boulder, CO, USA) was used to detect the extent of periosteal calcein labeling. Percent periosteal-labeled surface (Ps.LS) was determined as the ratio of Ps.LS to the middiaphyseal periosteal perimeter.

Noninvasive mouse tibia model

Eighteen adolescent female C57Bl/6J mice (10 weeks) underwent external loading of the right tibia using the noninvasive murine tibia loading device.(26) With the mouse anesthetized (2% isoflurane), the device secured the proximal tibia metaphysis from motion via a brass gripping cup. The tibia diaphysis then was placed under "cantilever" bending in the medial-lateral plane by applying force to the lateral distal tibia metaphysis via a computer-controlled linear force actuator. Mice were assigned randomly to three groups: (1) low magnitude (low, $n = 6$), (2) low magnitude rest-inserted (rest-inserted, $n = 6$), and (3) high magnitude (high, $n = 6$). The low-magnitude group underwent 100 cycles/day of a 0.25 N peak load, 1 Hz, 0.01/s strain rate trapezoidal waveform for 5 consecutive days (inducing 650 $\mu\epsilon$ peak normal strain at the middiaphysis in separate calibration mice). For the low-magnitude rest-inserted group, peak load (0.25 N) and peak strain rate (0.01/s) were equivalent to the low-magnitude group. However, instead of 100 daily load cycles, the rest-inserted mice were exposed to a 10-cycle/day regime with a 10-s pause inserted between each load cycle. The high-magnitude group underwent a 100-cycle/day 1-Hz regime with the peak load and strain rate doubled compared with the low-magnitude group (0.5 N; 0.02/s) and served as a positive control for an osteogenic response in the model (Fig. 1). The overall daily external loading period for the mice in all groups was 100 s. All animals were allowed 23 days of free cage activity after the 5-day loading regimen to facilitate consolidation of new bone. All mice received calcein injections (15 mg/kg intraperitoneally [ip]) on day 1 and day 26 to detect osteoblast activity over the course of the experiment. After death, on day 28, 100-μm-thick middiaphyseal cross-sections were taken from the right (experimental) and left (intact contralateral) tibias and were mounted unstained for evaluation of cross-sectional areal properties and dynamic indices of bone formation. Sections were imaged (100×) with identity blinded. On both the endocortical and periosteal surfaces, single-labeled surface (sLS), double-labeled surface (dLS), and interlabel thickness (Ir.L.Th) were measured. From these data, mineralizing surface (MS; MS = (dLS + sLS/)/bone surface [BS] * 100), mineral apposition rate (MAR; MAR = Ir.L.Th/interlabel time period [Ir.L.t]), and surface referent bone formation rate (BFR; BFR = MAR * MS/BS) were calculated.(27) Static measures of the periosteal envelope (periosteal area [Ps.Ar]) and endocortical envelope (endocortical area [Ec.Ar]) were used to determine cross-sectional cortical area (Ct.Ar). Animal-specific peak middiaphyseal strains induced at the initiation of the loading experiments were calculated using beam theory to apply end loading conditions established in separate calibration experiments via a combined strain gauging and finite element (FE) analysis approach.

Statistics

Nonparametric statistical comparisons were used to assess within-group and across-group treatment effects. Wilcoxon paired tests ($p = 0.05$, one-tailed) were used to distinguish differences between loaded bones and intact contralateral bones. Kruskal-Wallis tests ($p = 0.05$, two-tailed) were used to identify differences due to different loading regimes, with Mann-Whitney tests used as a post hoc follow-up ($p = 0.05$, two-tailed).

RESULTS

Avian ulna model

The loading regimens induced nearly identical mean (±SE) peak normal strains in the standard waveform group ($820 \pm 50\mu\varepsilon$) and the rest-inserted group (830 ± 60 $\mu\varepsilon$; $p = 0.40$). Only two of eight intact contralateral ulnas showed any periosteal labeling (both in the rest-inserted group). Averaged across all turkeys, $1.6 \pm 1.5\%$ of the periosteal surface was labeled in the intact bones. The standard loading waveform elicited a small but significant elevation in the Ps.LS compared with intact contralateral bones ($3.8 \pm 1.5\%$; $p = 0.03$; Fig. 2). The rest-inserted waveform was highly osteogenic ($21.9 \pm 4.5\%$; $p = 0.03$). The 5.8-fold increase in labeled surface elicited by the rest-inserted loading compared with standard loading was statistically significant ($p = 0.03$).

Noninvasive mouse tibia model

Peak longitudinal normal strains were equivalent in the low-magnitude and rest-inserted groups (680 ± 20 $\mu\varepsilon$ vs. $665 \pm 25\mu\varepsilon$; $p = 0.39$) and were doubled in the high-magnitude group ($1330 \pm 50\mu\varepsilon$). The young mice examined in this study exhibited active osteoblast activity on both endocortical and periosteal surfaces at the initiation of the study. None of the three loading regimens altered endocortical bone formation parameters compared with normal contralateral tibia (Table 1). In contrast, osteoblastic activity on the periosteum was significantly enhanced by both the high-magnitude and the rest-inserted regimes (Fig. 3). Histologically, new bone formation was lamellar, with no evidence of woven bone. Compared with paired intact tibia, periosteal MS was not significantly altered by low-magnitude loading (Fig. 4) but was significantly enhanced by high-magnitude ($p = 0.04$) and rest-inserted loading ($p = 0.01$). Likewise, periosteal MAR was not altered by low-magnitude loading but was significantly elevated by both high-magnitude ($p = 0.01$) and rest-inserted loading ($p = 0.01$; Fig. 4). As a result, periosteal BFR was significantly elevated in both high-magnitude ($p = 0.01$; 3.7-fold vs. paired contralateral tibia, 14.5-fold vs. low magnitude) and rest-inserted load groups ($p = 0.01$; 2.3-fold vs. paired contralateral tibia, 8.0-fold vs. low magnitude) but was not altered in the low-magnitude group (Fig. 4). Although both high-magnitude and rest-inserted loading were more stimulatory for osteoblasts than low-magnitude loading, no statistical differences were observed between high-magnitude and rest-inserted loading for any bone formation parameter. As compared with intact bones, both high-magnitude ($p = 0.05$) and rest-inserted ($p = 0.03$) loading induced small but significant increases in Ct.Ar (5.1% and 6.2%, respectively). Ct.Ar was achieved primarily via expansion of the periosteal envelope (Table 2).

DISCUSSION

We used two distinct in vivo models of bone adaptation to examine whether insertion of a brief rest interval between each load cycle enhances the osteogenic potential of low-magnitude mechanical loading. In the avian ulna model, the periosteum was quiescent under normal conditions. We found that low-magnitude locomotion-like loading only minimally influenced osteoblast activity. Surprisingly, insertion of a 10-s rest interval between each load cycle transformed the low-magnitude regimen into a potent anabolic stimulus. Using the noninvasive murine tibia-loading model, we found that low magnitude did not alter periosteal bone formation versus normal control bones. When a 10-s rest interval was inserted between each loading cycle, periosteal bone formation was significantly enhanced, despite a 10-fold reduction in daily load cycle number. Last, we found that the bone formation elicited by 10 cycles of rest-inserted loading was statistically comparable with that induced by a standard locomotion-like waveform 10-fold greater in cycle number and 2-fold greater in load magnitude and rate.

The ability of rest-inserted loading to significantly augment the osteogenic potential of low-magnitude loading in both adult and growing skeletons suggests promise as a potential strategy to build bone mass via exercise. However, a number of facets of this observation remain to be resolved before its successful application. First, the described studies used models of cortical bone adaptation. Augmentation of both trabecular and cortical bone would enhance most effectively bone structural properties, but it is not known whether rest-inserted loading will be similarly osteogenic for trabecular bone. To date, we have not attempted to optimize the rest interval. Our initial choice of a 10-s rest pause appears somewhat serendipitous because based on our preliminary reports,(28,29) a recent study using larger-magnitude loading protocols (about fourfold greater peak strain magnitude than the low-magnitude protocols used here) found that rest intervals of 3.5 s and 7 s were ineffective, but 14 s increased bone formation compared with repetitive loading regimes.(30) It remains to be determined whether optimal rest intervals are similar across species, different peak strain magnitudes, and different cycle durations. Also, it remains to be assessed whether rest-inserted loading will ultimately augment structural properties sufficiently to decrease fracture risk, because the initial studies described here assessed the ability of rest-inserted loading to initiate an osteogenic response (i.e., periosteal activation and bone formation). Extension of this response over weeks and months likely will be required to significantly enhance structural properties.

Although the data of this study do not specifically address the mechanism by which rest-inserted loading derived its potency, they circumstantially support the thesis that fluid flow near osteocytes mediates mechanotransduction within bone. In this context, we recently reported a numerical model of lacunocanalicular fluid flow, suggesting that load-induced fluid flows near osteocytes were reduced substantially (>45%) beyond the first few load cycles of repetitive locomotion-like mechanical loading.(24) Our physical interpretation of this phenomenon was related to the forced flow of viscous interstitial fluids through the fiber-filled canalicular annuli and the consequent "inertia" in the fluid flow. In the present in vivo studies, tissue deformations were identical for both standard locomotion-like loading and rest-inserted loading; yet, insertion of a rest interval activated a substantially larger proportion of the periosteum (turkey) and induced more bone formation (mice). These results suggest that rest-inserted loading may derive its efficacy from enhancing secondary stimuli induced when bone is loaded mechanically (i.e., stimuli other than deformation of the tissue). It is reasonable to assume that a 10-s rest interval would diminish inertial fluid flow effects associated with locomotion-like exercise that contains nonloaded periods only during the swing phase of gait. Thus, fluid flow near osteocytes (and associated processes such as shear stress, nutrient exchange, and convection of cytokines) likely were elevated in the rest-inserted regimes.

Alternatively (or additionally), the effectiveness of rest-inserted loading may arise from other distinct processes. For example, a substantial body of literature indicates that repetitive stimuli rapidly saturate cellular responses in various tissues(31–33) and that the response of bone to a few cycles of repetitive loading is similar to that achieved with orders of magnitude more load cycles.(25,34,35) Recent in vivo data confirm that bone becomes accommodated to repetitive loading, as separation of a 360-cycle daily loading protocol into 4 bouts of 90 cycles over the course of a day enhances the anabolic response of bone to mechanical loading.(36)

Although rest-inserted loading remains to be optimized, it represents a departure from established modalities of repetitively loading bone tissue. In both in vivo and in vitro models, mechanical stimuli such as increased strain magnitude(7,8) and rate,(37,38) loading frequency, (39) and fluid flow(40,41) have been shown potently osteogenic. In general, these investigations have established the paradigm that the greater the mechanical stimulus, the greater the response elicited from bone cells or bone tissue. Comparison of the standard low- and high-magnitude groups confirms this pattern of response in the murine tibia model. However, in the growing mouse, we found that 10 cycles of low-magnitude rest-inserted

loading substantially enhanced bone formation compared with control bones, while 100 cycles of an identical-magnitude repetitive loading without rest between cycles did not alter bone formation versus control bones. In addition, the amount of bone formation induced by 10 cycles of daily rest-inserted loading was not significantly different from that achieved by the positive control high-magnitude group exposed to twice the load magnitude and rate and 10 times the number of load cycles. The ability of rest-inserted loading to induce more bone formation (vs. low-magnitude loading) or equivalent bone formation (vs. high-magnitude loading) with less actual loading of bone (cycle number and/or magnitude, respectively) directly challenges the concept that high-magnitude, high-impact loading is required to build bone mass.

In this context, the broad relevance of these data lie with their potential to extend substantially the skeletal benefits of mild exercise. The ability to induce bone formation in growing or mature skeletons via low-magnitude nonimpact loading would make bone-building exercise accessible to all ages while minimizing injury risk. A number of possibilities might be explored readily to implement rest-inserted loading. Tai Chi, which already has been suggested to enhance balance in the elderly,(42) might be modified such that postures between movements are deliberately held for longer periods of time. Similarly, hand weights might be held in fixed positions between each load repetition to enhance bone mass in the upper extremities. With such ease of implementation, rest-inserted waveforms also might be combined with the low-magnitude high-frequency loading that is highly osteogenic for trabecular bone(39) as a means of focally enhanced bone structure at any skeletal site.

In summary, insertion of a 10-s rest interval between each load cycle transformed a low-magnitude minimally osteogenic loading regimen into a potent osteogenic stimulus in two distinct in vivo models of bone adaptation. We found that 10 cycles of low-magnitude loading per day interspersed with 10 s of rest induced equivalent bone formation as a regimen of 100 cycles/day of twice the strain magnitude and twice the strain rate. These studies with cortical bone emphasize that it should be possible to augment bone structure without subjecting an individual to high-magnitude high-impact loading. If so, low-magnitude or mild exercise regimes interspersed with rest intervals between load cycles may prove a safe and highly effective treatment for both acute (e.g., space induced) and chronic (e.g., paralysis or aging induced) bone loss.

References

1. Bass S, Delmas PD, Pearce G, Hendrich E, Tabensky A, Seeman E. The differing tempo of growth in bone size, mass, and density in girls is region-specific. J Clin Invest 1999;104:795–804. [PubMed: 10491415]

2. Hansen MA, Overgaard K, Riis BJ, Christiansen C. Role of peak bone mass and bone loss in postmenopausal osteoporosis: 12 year study. BMJ 1991;303:961–964. [PubMed: 1954420]

3. Hosking D, Chilvers CED, Christiansen C, Ravn P, Wasnich R, Ross P, McClung M, Balske A, Thompson D, Daley M, Yates AJ. Prevention of bone loss with alendronate in postmenopausal women under 60 years of age. N Engl J Med 1998;338:485–492. [PubMed: 9443925]

4. Sogaard CH, Mosekilde L, Thomsen JS, Richards A, McOsker JE. A comparison of the effects of two anabolic agents (fluoride and PTH) on ash density and bone strength assessed in an osteopenic rat model. Bone 1997;20:439–449. [PubMed: 9145241]

5. Finkelstein JS, Klibanski A, Arnold AL, Toth TL, Hornstein MD, Neer RM. Prevention of estrogen deficiency-related bone loss with human parathyroid hormone-(1–34): A randomized controlled trial. JAMA 1998;280:1067–1073. [PubMed: 9757854]

6. Cummings SR, Black DM, Nevitt MC, Browner WS, Cauley JA, Genant HK, Mascioli SR, Scott JC, Seeley DG, Sherwin R, Steiger P, Vogt TM. Appendicular bone density and age predict hip fracture in women. The Study of Osteoporotic Fractures Research Group [see comments]. JAMA 1990;263:665–668. [PubMed: 2404146]

7. Rubin CT, Lanyon LE. Regulation of bone mass by mechanical strain magnitude. Calcif Tissue Int 1985;37 (4):411–7. [PubMed: 3930039]

8. Turner CH, Forwood MR, Rho JY, Yoshikawa T. Mechanical loading thresholds for lamellar and woven bone formation. J Bone Miner Res 1994;9:87–97. [PubMed: 8154314]

9. Prince RL, Smith M, Dick IM, Price RI, Webb PG, Henderson NK, Harris MM. Prevention of postmenopausal osteoporosis. A comparative study of exercise, calcium supplementation, and hormone-replacement therapy. N Engl J Med 1991;325:1189–1195. [PubMed: 1922205]

10. Nelson ME, Fiatarone MA, Morganti CM, Trice I, Greenberg RA, Evans WJ. Effects of high-intensity strength training on multiple risk factors for osteoporotic fractures. A randomized controlled trial. JAMA 1994;272:1909–1914. [PubMed: 7990242]

11. Pruitt LA, Taaffe DR, Marcus R. Effects of a one-year high-intensity versus low-intensity resistance training program on bone mineral density in older women. J Bone Miner Res 1995;10:1788–1795. [PubMed: 8592957]

12. Doty SB. Morphological evidence of gap junctions between bone cells. Calcif Tissue Int 1981;33:509–512. [PubMed: 6797704]

13. Palumbo C, Palazzini S, Marotti G. Morphological study of intercellular junctions during osteocyte differentiation. Bone 1990;11:401–406. [PubMed: 2078434]

14. Knothe Tate ML, Steck R, Forwood MR, Niederer P. In vivo demonstration of load-induced fluid flow in the rat tibia and its potential implications for processes associated with functional adaptation. J Exp Biol 2000;203(Pt 18):2737–2745. [PubMed: 10952874]

15. Piekarski K, Munro M. Transport mechanism operating between blood supply and osteocytes in long bones. Nature 1977;269:80–82. [PubMed: 895891]

16. Zeng Y, Cowin SC, Weinbaum S. A fiber matrix model for fluid flow and streaming potentials in the canaliculi of an osteon. Ann Biomed Eng 1994;22:280–292. [PubMed: 7978549]

17. Klein-Nulend J, Semeins CM, Ajubi NE, Nijweide PJ, Burger EH. Pulsating fluid flow increases nitric oxide (NO) synthesis by osteocytes but not periosteal fibroblasts—correlation with prostaglandin upregulation. Biochem Biophys Res Commun 1995;217:640–648. [PubMed: 7503746]

18. Cheng B, Zhao S, Luo J, Sprague E, Bonewald LF, Jiang JX. Expression of functional gap junctions and regulation by fluid flow in osteocyte-like MLO-Y4 cells. J Bone Miner Res 2001;16:249–259. [PubMed: 11204425]

19. Gross TS, Srinivasan S. Association of osteoblastic activation with spatial strain gradients. Tran Orthop Res Soc 1998;44:944.

20. Qin YX, McLeod KJ, Guilak F, Chiang FP, Rubin CT. Correlation of bony ingrowth to the distribution of stress and strain parameters surrounding a porous-coated implant. J Orthop Res 1996;14:862–870. [PubMed: 8982127]

21. Cane V, Marotti G, Volpi G, Zaffe D, Palazzini S, Remaggi F, Muglia MA. Size and density of osteocyte lacunae in different regions of long bones. Calcif Tissue Int 1982;34:558–563. [PubMed: 6819077]

22. Michel CC. Capillary permeability and how it may change. J Physiol 1988;404:1–29. [PubMed: 3075669]

23. Zhu W, Lai WM, Mow VC. The density and strength of proteoglycan-proteoglycan interaction sites in concentrated solutions. J Biomech 1991;24:1007–1018. [PubMed: 1761579]

24. Srinivasan S, Gross TS. Canalicular fluid flow induced by bending of a long bone. Med Eng Phys 2000;22:127–133. [PubMed: 10854966]

25. Rubin CT, Lanyon LE. Regulation of bone formation by applied dynamic loads. J Bone Joint Surg Am 1984;66:397–402. [PubMed: 6699056]

26. Gross TS, Srinivasan S, Liu C, Clemens TL, Bain SD. Non-invasive loading of the murine tibia: An in vivo model for study of mechanotransduction. J Bone Miner Res 2002;17:493–501. [PubMed: 11874240]

27. Parfitt AM, Drezner MK, Glorieux FH, Kanis JA, Malluche H, Meunier PJ, Ott SM, Recker RR. Bone histomorphometry: Standardization of nomenclature, symbols, and units. Report of the ASBMR Histomorphometry Nomenclature Committee. J Bone Miner Res 1987;2:595–610. [PubMed: 3455637]

28. Srinivasan S, Gross TS. Intermittent rest enhances osteoblastic activation induced by mechanical loading. Trans Orthop Res Soc 2000;25:628.

29. Srinivasan S, Weimer DA, Liu CC, Bain SD, Gross TS. The osteogenic potential of rest-inserted loading. Trans Orthop Res Soc 2001;26:325.

30. Robling AG, Burr DB, Turner CH. Recovery periods restore mechanosensitivity to dynamically loaded bone. J Exp Biol 2001;204(Pt 19):3389–3399. [PubMed: 11606612]

31. Davies PF, Dewey CF Jr, Bussolari SR, Gordon EJ, Gimbrone MA Jr. Influence of hemodynamic forces on vascular endothelial function. In vitro studies of shear stress and pinocytosis in bovine aortic cells. J Clin Invest 1984;73:1121–1129. [PubMed: 6707208]

32. Chitwood RA, Jaffe DB. Calcium-dependent spike-frequency accommodation in hippocampal CA3 nonpyramidal neurons. J Neurophysiol 1998;80:983–988. [PubMed: 9705484]

33. Cordoba-Rodriguez R, Moore KA, Kao JP, Weinreich D. Calcium regulation of a slow post-spike hyperpolarization in vagal afferent neurons. Proc Natl Acad Sci USA 1999;96:7650–7657. [PubMed: 10393875]

34. Unemura Y, Ishiko T, Yamauchi T, Kurono M, Mashiko S. Five jumps per day increase bone mass and breaking force in rats. J Bone Miner Res 1997;12:1480–1485. [PubMed: 9286765]

35. Turner CH. Three rules for bone adaptation to mechanical stimuli. Bone 1998;23:399–407. [PubMed: 9823445]

36. Robling AG, Burr DB, Turner CH. Partitioning a daily mechanical stimulus into discrete loading bouts improves the osteogenic response to loading. J Bone Miner Res 2000;15:1596–1602. [PubMed: 10934659]

37. O'Connor JA, Lanyon LE, MacFie H. The influence of strain rate on adaptive bone remodelling. J Biomech 1982;15:767–781. [PubMed: 7153230]

38. Mosley JR, Lanyon LE. Strain rate as a controlling influence on adaptive modeling in response to dynamic loading of the ulna in growing male rats. Bone 1998;23:313–318. [PubMed: 9763142]

39. Rubin C, Turner AS, Bain S, Mallinckrodt C, McLeod K. Anabolism. Low mechanical signals strengthen long bones. Nature 2001;412:603–604. [PubMed: 11493908]

40. Reich KM, Gay CV, Frangos JA. Fluid shear stress as a mediator of osteoblast cyclic adenosine monophosphate production. J Cell Physiol 1990;143:100–104. [PubMed: 2156870]

41. Klein-Nulend J, van der Plas A, Semeins CM, Ajubi NE, Frangos JA, Nijweide PJ, Burger EH. Sensitivity of osteocytes to biomechanical stress in vitro. FASEB J 1995;9:441–445. [PubMed: 7896017]

42. Wolfson L, Whipple R, Derby C, Judge J, King M, Amerman P, Schmidt J, Smyers D. Balance and strength training in older adults: Intervention gains and Tai Chi maintenance [see comments]. J Am Geriatr Soc 1996;44:498–506. [PubMed: 8617896]
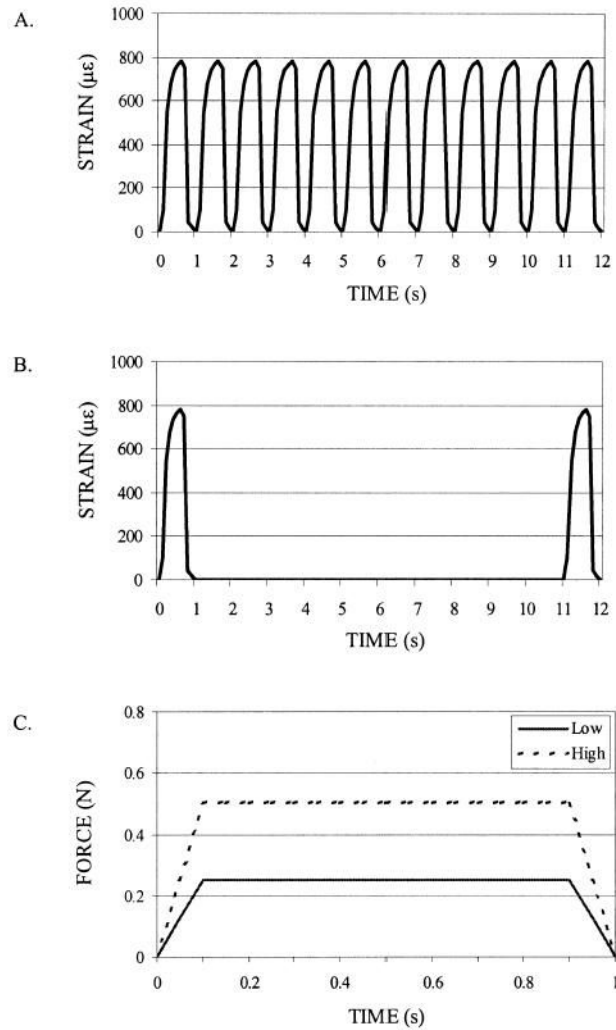
FIG. 1.
The (A) standard waveform and (B) rest-inserted waveform were identical in magnitude and total cycle number in the avian ulna study (illustrated via middiaphyseal normal strains). They differed only by the 10-s pause inserted between each loading cycle of the rest-inserted waveform. The first 12 s of each regimen is illustrated. (C) For the murine tibia study, single load cycles for the low- and high-magnitude groups are illustrated via applied load waveforms. The rest-inserted load waveform was identical to that of the low-magnitude group, with 10 s of rest inserted between each cycle.
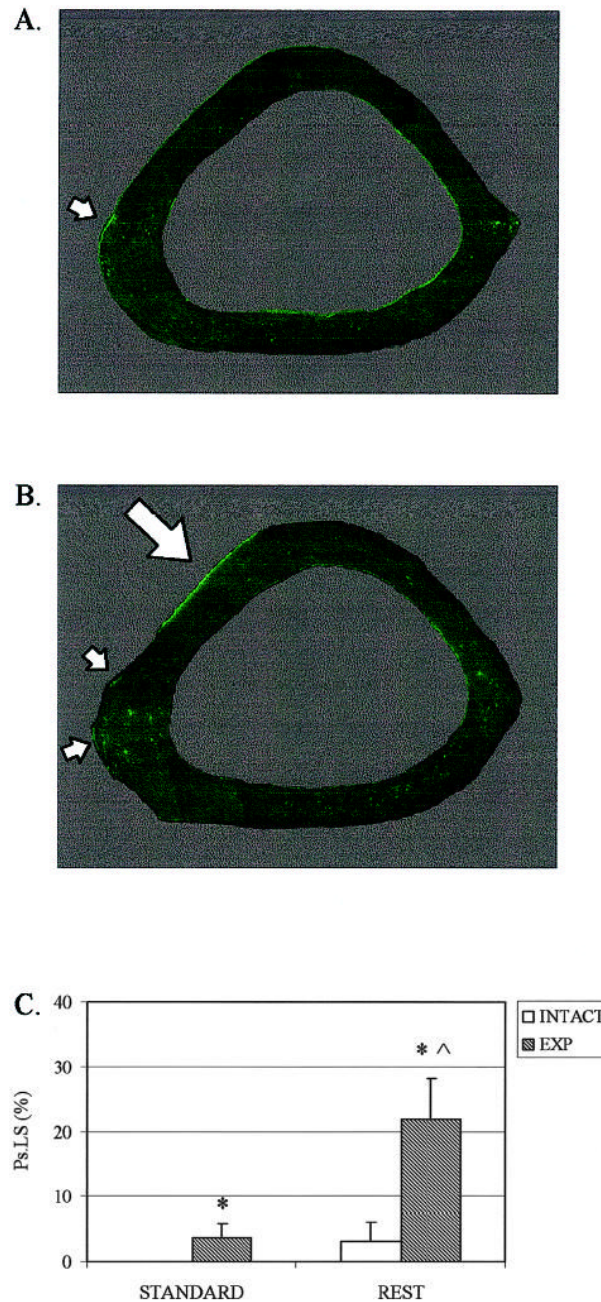
FIG. 2.
(A) Composite fluorescent micrograph of the ulna middiaphysis illustrating the minimal Ps.LS induced by a 1-week application of the standard waveform. (B) In contrast, substantial Ps.LS was evident on ulna loaded using the rest-inserted protocol (arrows highlighting calcein labeling). (C) Both the low-magnitude standard waveform ($p = 0.03$) and the rest-inserted waveform ($p = 0.03$) significantly elevated Ps.LS versus intact contralateral bones (*). Ps.LS induced by rest-inserted loading was, in turn, significantly greater than that induced by the standard waveform ($p = 0.03$, ∧).
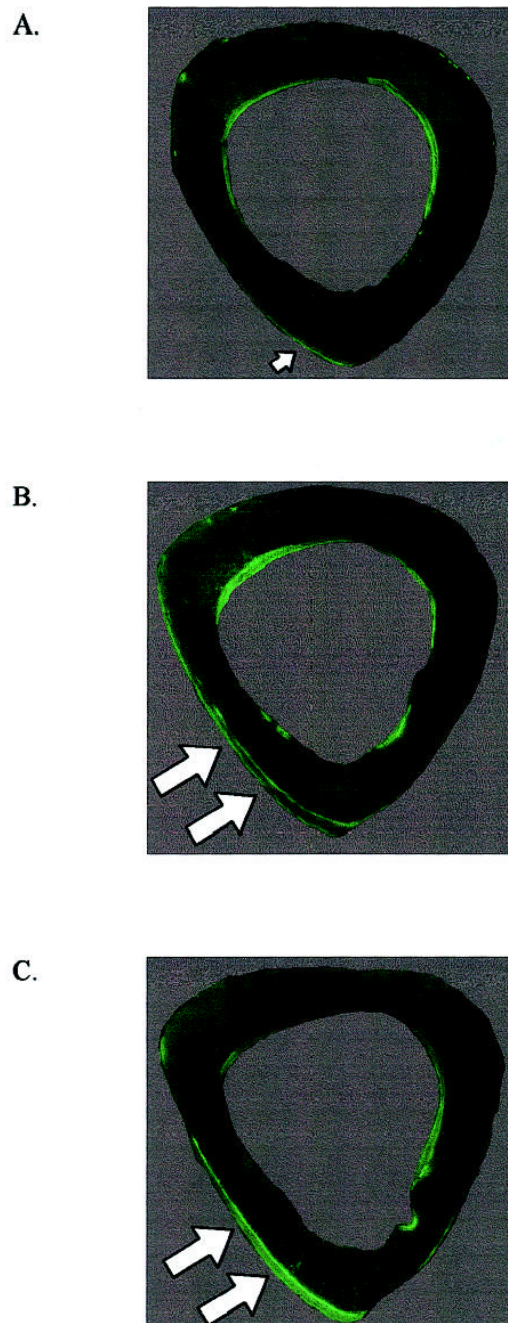
A.

B.

C.

FIG. 3.
Composite fluorescent micrographs of the mouse midshaft illustrate (A) minimal periosteal bone formation in response to the low-magnitude regimen, and (B) substantial periosteal bone formation stimulated by the high-magnitude and (C) rest-inserted regimens (arrows). Endocortical bone formation was similar for each group and no different from that observed in the intact contralateral tibia.
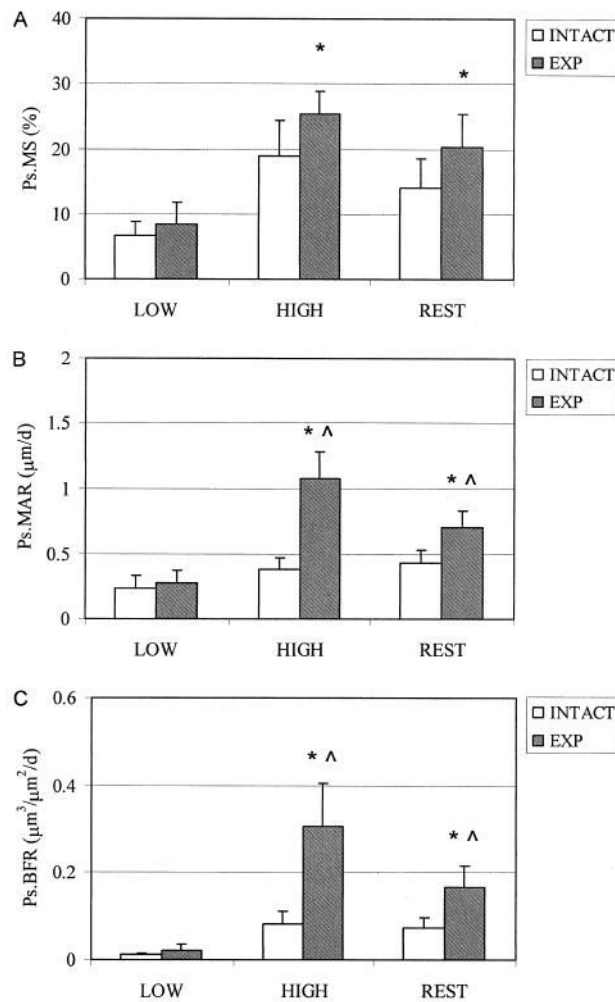
FIG. 4.
Periosteal bone formation parameters at the tibia midshaft in response to low-magnitude, high-magnitude, and low-magnitude rest-inserted loading. Low magnitude loading did not significantly alter (A) MS, (B) MAR, or (C) BFR compared with the intact contralateral tibia. Both high-magnitude and rest-inserted loading significantly enhanced these parameters (*). In addition, both high-magnitude and rest-inserted loading induced significantly greater mineral apposition and bone formation compared with the low-magnitude loading (∧). No statistical differences were observed between high-magnitude and rest-inserted loading.

Table 1

Mean (±SE) Endocortical Bone Formation Data From Noninvasive Loading of the Mouse Tibia

		Ec.MS (%)	Ec.MAR (µm/day)	Ec.BFR ($\mu m^3/\mu m^2$ per day)
Low	Intact	51.5 (±6.18)	0.85 (±0.17)	0.45 (±0.10)
	Load	61.0 (±8.72)	0.82 (±0.11)	0.55 (±0.13)
High	Intact	45.3 (±3.23)	0.71 (±0.08)	0.33 (±0.05)
	Load	37.3 (±5.50)	0.85 (±0.12)	0.33 (±0.06)
Rest	Intact	45.0 (±5.06)	0.80 (±0.12)	0.36 (±0.06)
	Load	40.2 (±5.72)	0.87 (±0.13)	0.36 (±0.07)

No significant differences were noted.

Low, low-magnitude loading group; high, high-magnitude loading group; rest, rest-inserted loading group; intact, intact left tibia; load, experimentally loaded right tibia.

Table 2

Mean (±SE) Cross-Sectional Areal Data From Noninvasive Loading of the Mouse Tibia

		$Ps.Ar\ (mm^2)$	$Ec.Ar\ (mm^2)$	$Ct.Ar\ (mm^2)$
Low	Intact	0.889 (±0.036)	0.399 (±0.025)	0.491 (±0.013)
	Load	0.880 (±0.018)	0.385 (±0.017)	0.495 (±0.006)
High	Intact	0.840 (±0.022)	0.347 (±0.013)	0.493 (±0.012)
	Load	**0.870 (±0.023)**	0.352 (±0.013)	**0.518 (±0.011)**
Rest	Intact	0.857 (±0.026)	0.390 (±0.014)	0.466 (±0.012)
	Load	0.898 (±0.022)	0.403 (±0.015)	**0.495 (±0.009)**

Significant differences are in bold.

Low, low-magnitude loading group; high, high-magnitude loading group; rest, rest-inserted loading group; intact, intact left tibia; load, experimentally loaded right tibia; bold, loaded tibias significantly increased versus intact tibias ($p < 0.05$).